Pyroptosis in Alzheimer's disease: cell type-specific activation in microglia, astrocytes and neurons

Authors

Sebastiaan Moonen[1,2,3], Marta J. Koper[1,2,3], Evelien Van Schoor[1,3,4], Jolien M. Schaeverbeke[5], Rik Vandenberghe[5,6], Christine A.F. von Arnim[7,8], Thomas Tousseyn[9], Bart De Strooper[2,3,10], Dietmar R. Thal[1,9]

Affiliations

1. Laboratory for Neuropathology, Department of Imaging and Pathology, Leuven Brain Institute (LBI), KU Leuven (University of Leuven), Leuven, Belgium
2. Laboratory for the Research of Neurodegenerative Diseases, Department of Neurosciences, Leuven Brain Institute (LBI), KU Leuven (University of Leuven), 3000 Leuven, Belgium
3. Vlaams Instituut voor Biotechnologie (VIB) Center for Brain and Disease Research, VIB, Leuven, Belgium
4. Laboratory for Neurobiology, Department of Neurosciences, Leuven Brain Institute (LBI), KU Leuven (University of Leuven), Leuven, Belgium
5. Laboratory for Cognitive Neurology, Department of Neurosciences, Leuven Brain Institute (LBI), KU Leuven (University of Leuven), Leuven, Belgium
6. Department of Neurology, University Hospital Leuven, Leuven, Belgium
7. Department of Neurology, University of Ulm, Ulm, Germany
8. Department of Geriatrics, University Medical Center Göttingen, Göttingen, Germany
9. Department of Pathology, University Hospital Leuven, Leuven, Belgium
10. UK Dementia Research Institute, Institute of Neurology, University College London, London, UK

Corresponding authors

Dietmar R. Thal
Laboratory for Neuropathology
O&N IV Herestraat 49 - bus 1032
3000 Leuven
Tel.: 0032/16/3-44047
E-mail address: dietmar.thal@kuleuven.be

Sebastiaan Moonen
Laboratory for Neuropathology
O&N IV Herestraat 49 - bus 1032
3000 Leuven
Tel.: 0032/16/3-44047
E-mail address: bas.moonen@kuleuven.be

Number of figures (main): 7

Number of figures (supplementary): 6

Number of tables (supplementary): 4

Ethical approval

Human post-mortem brain tissue was collected in accordance with the applicable laws in Belgium (UZ Leuven) and Germany (Ulm). The recruitment protocols for the collection of human brains were approved by the ethical committees of the UZ Leuven (Belgium; S-59292, S-52791) and the University of Ulm (Germany; 54/08). This study was approved by the UZ Leuven ethical committee (Leuven, Belgium; S-64378).

Availability of data and material

All relevant data generated and analyzed in this study are available in this manuscript, supplementary information or upon reasonable request.

Keywords

Alzheimer's disease, neuroinflammation, inflammasome, pyroptosis, cell death

ABSTRACT

The major neuropathological hallmarks of Alzheimer's disease (AD) are amyloid β (Aβ) plaques and neurofibrillary tangles (NFT) consisting of hyperphosphorylated Tau protein (pTau), accompanied by neuroinflammation and neuronal loss. Increasing evidence is emerging for the activation of the canonical NLRP3 inflammasome in AD, a key innate immune sensor, contributing to Aβ and pTau pathology in transgenic mice modeling these pathologies. However, the mechanisms leading to neuronal loss in AD and the involvement of glial cells in these processes are still not clear. The aim of this study was to investigate the activation of pyroptosis, a pro-inflammatory mechanism of regulated cell death downstream of the inflammasome, in the brains of AD patients. Using immunohistochemistry, we investigated the expression of cleaved GSDMD, the pyroptosis effector protein, as well as the NLRP3 inflammasome-forming proteins, in the medial temporal lobe of 23 symptomatic AD, 25 pathologically defined preclinical AD (p-preAD) and 22 non-demented control cases. Expression of cleaved GSDMD was found in microglia, but also astrocytes and few pyramidal neurons in the hippocampus and the temporal cortex. From the cell types expressing cleaved GSDMD, only microglia expressed all NLRP3 inflammasome-forming proteins. Cleaved GSDMD-positive astrocytes and neurons exhibited caspase-8 and caspase-4 respectively, potentially indicating alternative pathways for GSDMD cleavage. Brains of AD patients exhibited increased numbers of cleaved GSDMD-positive cells. Cleaved GSDMD-positive microglial cells and astrocytes were found in close proximity to Aβ plaques, while cleaved GSDMD-positive neurons were devoid of NFTs. In CA1, NLRP3-positive microglial cells and cleaved GSDMD-positive neurons were associated with local neuronal loss, indicating a possible contribution of NLRP3 inflammasome and pyroptosis activation to neuronal loss in AD. Taken together, our results suggest a cell type-specific activation of pyroptosis in AD via pathways involving the canonical or non-canonical inflammasome.

INTRODUCTION

More than 50 million people worldwide suffer from dementia, of which 60-70% have Alzheimer's disease (AD) [63]. AD is characterized by cerebral atrophy with underlying neuronal loss, leading to progressive deterioration of memory and cognitive function [30, 34, 65]. Symptoms are generally preceded by a preclinical stage of 10 to 30 years during which pathological changes already occur [34, 52]. The deposition of extracellular plaques mainly consisting of insoluble amyloid β protein (Aβ) and the formation of intraneuronal neurofibrillary tangles (NFTs) comprising hyperphosphorylated Tau protein (pTau) are considered the major neuropathological hallmarks of AD [4]. These lesions are associated with chronic neuroinflammation mediated by reactive microglia and astrocytes, which is accompanied by the release of inflammatory cytokines [28, 38]. These reactive glial cells are known to accumulate around Aβ plaques, and correlate with NFT burden [14, 47].

One of the pathways leading to the release of inflammatory cytokines is activation of the *NOD-, LRR- and pyrin domain-containing 3* (NLRP3) inflammasome, a key innate immune sensor [20]. During NLRP3 inflammasome activation, the receptor protein NLRP3 forms a multi-protein complex with *apoptosis-associated speck-like protein* (ASC) and caspase-1 [32]. Subsequently, caspase-1 is cleaved and activated, in turn cleaving the inflammatory cytokines pro-IL-1β and pro-IL-18, yielding their biologically active forms [15, 31, 48]. Additionally, caspase-1 cleaves Gasdermin D (GSDMD), releasing its N-terminal fragment (GSDMD-NT) [49]. These cleaved GSDMD peptides oligomerize and form pores in the plasma membrane, eventually leading to pyroptotic cell death and the release of mature IL-1β and IL-18 [31, 44]. This intrinsically pro-inflammatory type of cell death is marked by DNA fragmentation as well as nucleus and chromatin condensation, and is accompanied by the release of cellular content [17, 44, 49]. Besides NLRP3 inflammasome-dependent pyroptosis activation, this cell death mechanism can also be activated directly via caspase-4 during non-canonical inflammasome activation [27] or caspase-8 [43].

Increasing evidence is emerging for the activation of the NLRP3 inflammasome in AD, including elevated expression of activated caspase-1 in the frontal cortex and hippocampus of AD patients [19],

and contribution of NLRP3 inflammasome activation to Aβ and pTau pathology in transgenic mice [19, 20, 25]. On the other hand, Aβ and pTau pathology were shown to drive the activation of the NLRP3 inflammasome [25, 54], suggesting a vicious cycle of increasing pathology and neuroinflammation. It has been reported that microglia, astrocytes and neurons express components of the NLRP3 inflammasome [22, 25, 66], although it is not yet clear if these cell types exhibit NLRP3 inflammasome-driven pyroptosis. Interestingly, NLRP3 inflammasome activation was recently linked to microglial pyroptotic cell death and reduced Aβ clearance *in vitro* [9]. However, the expression of the pyroptotic effector cleaved GSDMD has not yet been investigated in AD. Although evidence for the activation of the NLRP3 inflammasome in AD and its contribution to AD-related pathology is strong [19, 25], it remains unclear whether downstream pyroptosis activation occurs in human AD patients, contributing to AD pathophysiology, and which cell types are involved.

Here, we analyzed the activation of pyroptosis, as well as the canonical NLRP3 and non-canonical inflammasome, in different cell types in the medial temporal lobe (MTL) of human AD patients. We investigated the expression of pyroptosis-related proteins (i.e. cleaved GSDMD and IL-18), the components of the NLRP3 inflammasome (i.e. ASC, NLRP3 and caspase-1), as well as caspase-4 and caspase-8, in microglia, astrocytes and neurons, and their association with AD pathology. Our findings indicate differential activation of pyroptosis in a cell type-specific manner in AD patients. The expression of proteins involved in NLRP3 inflammasome and pyroptosis activation correlated with neuronal loss in AD, potentially indicating a contribution of inflammasome- and pyroptosis-activation to neuronal death.

MATERIALS AND METHODS

Human autopsy cases

Brain tissue samples from 70 patients were included in this study (**Suppl. Table 1**). Selection criteria were the absence of an encephalitis or meningitis and (a) meeting the criteria for symptomatic AD, i.e. clinical signs of dementia and intermediate-high degrees of AD neuropathological changes, (b)

exhibiting AD neuropathological changes without clinical signs of dementia indicative for pathologically-defined preclinical AD (p-preAD) [40], or (c) absence of dementia and AD neuropathological changes. Autopsies were performed in university or municipal hospitals in Belgium (Leuven) and Germany (Bonn, Ulm and Offenbach) in accordance with the applicable laws. Informed consent was obtained following local legislation. The recruitment protocols for the collection of human brains were approved by the ethical committees of the UZ Leuven (Belgium) and the University of Ulm (Germany). Tissue samples were taken during autopsy. The right hemisphere of the cerebrum and cerebellum as well as right half of the brainstem were dissected for gross neuropathological assessment and stored at -80 °C. The left cerebral and cerebellar hemispheres together with the left half of the brainstem were fixed in 4 % aqueous or phosphate-buffered formaldehyde for 2-4 weeks, followed by dissection and gross neuropathological assessment. Tissue samples from frontal, parietal, and occipital lobe (Area 17), cingulate gyrus, hippocampus with temporal cortex, entorhinal cortex, hypothalamus, basal ganglia, amygdala, basal nucleus of Meynert, thalamus, midbrain, pons, medulla oblongata, and cerebellum were collected. The clinical Dementia Rating (CDR) score [23] was retrospectively assessed based upon clinical files as previously described [18], reflecting the stage of cognitive and functional impairment of patients. The use of human brain samples in the context of this study was approved by the UZ Leuven ethical committee (Leuven, Belgium).

Neuropathology

Samples from all regions were embedded in paraffin and microtomed at 5 µm. Tissue was mounted on Flex IHC adhesive microscope slides (Dako, Glostrup, Denmark) and dried at 55 °C. Sections were stained with hematoxylin and eosin for diagnostic purposes. Post-mortem neuropathological assessment of AD pathology was performed based on standardized clinicopathological criteria, including Aβ plaque deposition in the medial temporal lobe (AβMTL phase) determined by Aβ immunohistochemistry [57, 58], the distribution of NFTs in the brain (Braak NFT stage) [2, 3] and neuritic plaque frequency (the Consortium to Establish a Registry for AD (CERAD) score) based on pTau immunohistochemistry [36]. The National Institute of Aging-Alzheimer Association (NIA-AA) score was

determined based on the AβMTL phase, Braak-NFT stage and CERAD score, reflecting the degree of AD pathology [24]. The GVD stage based on the presence of the necroptotic cell death effector pMLKL within the vacuoles of granulovacuolar degeneration (GVD) was determined according to previously described criteria [30, 59]. Cases were classified into three groups based on the clinical and post-mortem neuropathological diagnosis: (1) AD = intermediate-high NIA-AA score, signs of cognitive decline (CDR ≥ 0.5); (2) p-preAD = low–high NIA-AA score, no signs of cognitive decline (CDR = 0); and (3) non-AD = no signs of AD pathology (NIA-AA score = 0), no signs of cognitive decline (CDR = 0). Primary age-related tauopathy (PART) [7] was diagnosed in four non-AD control cases. Relevant clinicopathological characteristics of the cases included in this study are summarized in **Suppl. Table 1.**

Chromogen immunohistochemistry

The expression of NLRP3, ASC, caspase-1, cleaved GSDMD and IL-18 was examined in tissue sections of the MTL covering the hippocampus and temporal neocortex (Brodmann area 36). An overview of the primary antibodies and their respective dilutions used for the immunohistochemical analysis can be found in **Suppl. Table 2**. Paraffin-embedded tissue sections were processed and stained using a Leica BOND-MAX Automated IHC/ISH Stainer (Leica Biosystems, Wetzlar, Germany) with the Bond Polymer Refine Detection kit (DS9800, Leica Biosystems) according to the manufacturer's protocol. Briefly, tissue sections were deparaffinized and chemically treated for epitope retrieval (pH 6.1). Hydrogen peroxide was used to quench activity of endogenous peroxidase. Tissue sections were then incubated with primary antibodies for 30 min, followed by Horseradish Peroxidase (HRP)-labelled secondary antibodies. The substrate chromogen 3,3'-Diaminobenzidine tetrahydrochloride hydrate (DAB) was used to visualize the complex, followed by counterstaining with hematoxylin. After dehydration using an autostainer (Leica Biosystems), sections were mounted using an automated cover-slipper (Leica Biosystems) and Leica CV mount (Leica Biosystems). Images were taken with a Leica DFC7000 T camera (Leica Microsystems, Wetzlar, Germany) on a Leica DM2000 LED light

microscope (Leica Microsystems). Image processing was performed with ImageJ software (National Institutes of Health, Bethesda, USA) and Inkscape (https://inkscape.org/).

Quantification of immunoreactive cells

Immunoreactive microglial cells, astrocytes and neurons in the first sector of the *cornu ammonis* (CA1) within the hippocampus and in the temporal neocortex of Brodmann area 36 were quantified on DAB-stained tissue sections. Only regions lacking infarcts, microinfarcts or bleedings were considered for quantification. Morphological criteria for positive cells were determined prior to quantification. Cell types were distinguished based on cell type-specific cytological features as described by García-Cabezas *et al* [11], in combination with the staining pattern of the proteins of interest, as documented in **Suppl. Fig. 1**. For quantifications of immunoreactive microglial cells and astrocytes, three or five consecutive images were taken at x40 magnification (0.23 x 0.31 mm) of CA1 and cross-section of the temporal cortex (layer I-VI), respectively, using a Leica DM2000 LED microscope (Leica Microsystems). For neuronal counts, three consecutive images were taken at x20 magnification (0.46 x 0.62 mm) of CA1 and layer III of the temporal cortex, as described by Koper *et al* [30]. Positive cells were classified as microglial cells, astrocytes and neurons and counted manually using ImageJ software.

Immunofluorescence

Colocalization of inflammasome, pyroptosis, cell-type specific proteins and AD pathology was investigated using multiple labelling immunofluorescence. The microglial cell marker *ionized calcium binding adaptor molecule 1* (IBA1) and the astrocyte marker *glial fibrillary acidic protein* (GFAP) were used as cell-type specific markers. Anti-$A\beta_{17-24}$ (clone 4G8) and anti-pTau (S202/T205; clone AT8) were used to detect Aβ and pTau pathology respectively. Paraffin-embedded tissue sections comprising the hippocampal formation and temporal neocortex (Brodmann area 36) were deparaffinized using an autostainer (Leica Biosystems). Pretreatment was performed using a PT Link module (pH 6.1, Dako). Incubation with primary antibodies derived from different host species was done overnight in a humid chamber at room temperature (RT), followed by 90 min incubation with carbocyanine 2 (Cy2)/Alexa

488, Cy3 or Cy5 labeled secondary antibodies (Jackson ImmunoResearch Ltd, West Grove, USA). To combine two primary antibodies derived from the same host species, a modified staining protocol was used to avoid cross-reactivity of secondary antibodies, as previously described [30]. Briefly, incubation of the first primary antibody was performed as described above. The second primary antibody was incubated with donkey anti-rabbit Fab fragments (2 µg Fab fragment per 1 µg primary antibody, Jackson ImmunoResearch) conjugated to a Cy2 or Cy3 dye for 20 min. Normal rabbit serum (Jackson ImmunoResearch) was added for another 10 min to capture unbound Fab fragments (10 µl of serum per 1 µg Fab fragment). After incubation with normal donkey serum (Jackson ImmunoResearch) for 10 min, the mixture was added to the slides and left to incubate overnight in a humid chamber at room temperature (RT). All antibodies with their respective dilutions can be found in **Suppl. Table 2**. After incubation with TrueBlack Lipofuscin Autofluorescence Quencher (Biotium, Fremont, USA) for 30 s, tissue sections were mounted manually with ProLong Gold Antifade Mountant with DAPI (Thermo Fisher Scientific, Rockford, USA) for nuclear counterstaining. Images of immunofluorescence stainings were captured using a Nikon A1R laser scanning confocal system coupled to a Nikon Eclipse Ti inverted microscope (Nikon Instruments Inc., Melville, USA) using NIS-Elements (Nikon Instruments Europe B.V., Amstelveen, The Netherlands). Image processing was performed using ImageJ software.

Statistical analyses

GraphPad Prism (GraphPad, San Diego, USA) was used for analysis of variance. One-way ANOVA or the non-parametric equivalent Kruskal-Wallis test was performed followed by Tukey's or Dunn's multiple comparisons test, respectively, to assess significance of inter-group differences. Statistical significance was considered at $p < 0.05$. Partial correlation analysis was performed using IBM SPSS Statistics software (IBM, Armonk, USA). Correlation matrices, controlled for age and sex, were separately calculated for neuronal density in the hippocampal sector CA1 and in layer III of the temporal cortex, together with cleaved GSDMD-positive microglial cells, astrocytes and neurons, NLRP3- and Caspase-1-positive microglial cells, AβMTL phase, Braak NFT stage, CERAD, NIA-AA and CDR score, pMLKL-GVD stage. Post-mortem interval (PMI) was included to control for the effect of post-mortem delay on the

investigated variables. Variables that showed significant correlation with neuronal density in CA1 and/or layer III of the temporal cortex were further used for hierarchical regression analysis using R statistical software [45]. Repeated *k*-fold cross-validated models were computed using the R package *caret* (http://topepo.github.io/caret/index.html). For this, the data was randomly split into *k*-subsets, with *k* set to 10 with three repeats. Starting from a base model including age and sex, variables were added one by one according to decreasing correlation value. Models were compared pairwise to obtain the regression model that resulted in the lowest test sample Root Mean Squared Error (RMSE) and highest *R*-squared, indicators of model fit.

RESULTS

To investigate pyroptosis activation in AD, we performed immunohistochemical analyses on post-mortem brain tissue derived from the MTL of 23 symptomatic AD patients, 25 p-preAD [40] showing AD pathology but no overt clinical symptoms of dementia, and 22 non-demented control cases (non-AD) without signs of AD pathology and dementia. The CA1 region within the hippocampus was selected as a representative region for AD related cell loss [65], together with the temporal cortex. This gives the opportunity to analyze regions that are involved at different time points in the progression of the AD hallmark pathologies, Aβ plaques and NFTs [2, 57]. We observed expression of cleaved GSDMD in 19 (out of 23) AD, 17 (out of 25) p-preAD and 12 (out of 22) non-AD cases. The expression of cleaved GSDMD varied in different cell types, and in the distinct regions of the brain.

Expression of NLRP3 inflammasome and pyroptosis-related proteins in microglia of AD brain

Microglia exhibited expression of all proteins forming the NLRP3 inflammasome (ASC, NLRP3, caspase-1), as well as the pyroptosis effector proteins cleaved GSDMD and IL-18, in CA1 and the temporal cortex (**Fig. 1a**). To confirm the expression of the NLRP3 inflammasome and pyroptosis-related proteins in microglia, we performed multiple-label immunofluorescence using the microglial cell marker IBA1. The expression of ASC, NLRP3, caspase-1, cleaved GSDMD and IL-18 was observed in IBA1-positive cells, confirming expression in microglia (**Fig. 1b**). Cleaved GSDMD-positive microglia

primarily showed an enlarged cytoplasm and few processes and branches or few processes and no branches identified as amoeboid microglia, indicative of a reactive state [55].

Using immunohistochemically-stained tissue sections, cleaved GSDMD-positive microglial cells were quantified in CA1 and the temporal cortex. Microglia in CA1 were immunoreactive to cleaved GSDMD in 15 (out of 23) AD, 11 (out of 25) p-preAD and 5 (out of 22) non-AD cases. In the temporal cortex, cleaved GSDMD-positive microglia were observed in 16 AD, 13 p-preAD and 6 non-AD cases. Morphologically, the immunostaining pattern of microglial cleaved GSDMD showed cytoplasmic, often granular staining (**Suppl. Fig. 1a**). In CA1, a significant increase in cleaved GSDMD-positive microglial cells was observed in the AD group (15.3 ± 4.1 cells/mm^2) compared to the non-AD group (2.1 ± 1 cells/mm^2, p = 0.0036) (**Fig 1c**). Overall, the number of cleaved GSDMD-positive microglial cells increased with AD progression. Similar to CA1, cleaved GSDMD-positive microglial cells in the temporal cortex were increased in AD cases (4.7 ± 1.1 cells/mm^2) compared to non-AD cases (1.2 ± 0.5 cells/mm^2, p = 0.0187) (**Fig 1d**).

Additionally, we quantified microglial cells positive for the components of the NLRP3 inflammasome, and IL-18, in CA1 and the temporal cortex. High numbers of ASC-positive microglial cells were observed in both investigated regions across all groups (**Suppl. Fig. 2a,e**), suggesting physiological expression of ASC. In AD brain, NLRP3-positive microglial cells were increased in CA1 (8.9 ± 2.1 cells/mm^2, p = 0.0340) (**Suppl. Fig. 2b**) and the temporal cortex (18.5 ± 3 cells/mm^2, p = 0.0013) (**Suppl. Fig. 2f**) compared to non-AD brain (2.9 ± 0.9 cells/mm^2 and 6.1 ± 1.9 cells/mm^2 respectively), while no significant differences were observed in the number of caspase-1-positive microglial cells (**Suppl. Fig. 2c,g**). Finally, IL-18-positive microglial cells were increased in the CA1 region of p-preAD (40.4 ± 6.1 cells/mm^2, p = 0.0218) and AD cases (41.7 ± 7.2 cells/mm^2, p = 0.0370) compared to non-AD cases (**Suppl. Fig. 2d,h**).

Expression of cleaved GSDMD and caspase-8 in astrocytes of AD brain

In contrast to the expression of all NLRP3 inflammasome forming proteins in microglia, astrocytes in CA1 and temporal cortex exhibited NLRP3 and cleaved GSDMD, but no ASC, caspase-1 or IL-18 (**Fig. 2a**). Immunofluorescence stainings of CA1 showed expression of NLRP3 and cleaved GSDMD in GFAP-positive cells, confirming expression in astrocytes (**Fig. 2b**). Cleaved GSDMD-positive astrocytes showed a hypertrophic morphology with an enlarged cytoplasm, few processes and branches, representing a reactive morphology [1].

Quantifications of cleaved GSDMD-positive astrocytes in CA1 and the temporal cortex were performed on immunohistochemically-stained tissue sections, in a similar manner as for microglia. In CA1, astrocytes showed expression of cleaved GSDMD in 11 (out of 23) AD, 6 (out of 25) p-preAD and 2 (out of 22) non-AD cases. In the temporal cortex, cleaved GSDMD-positive astrocytes were observed in 12 AD, 11 p-preAD and 6 non-AD cases. Similar to the expression of cleaved GSDMD in microglia, the immunostaining pattern in astrocytes was cytoplasmic, often with a granular appearance, more uniformly distributed across the cytoplasm than in microglia (**Suppl. Fig. 1b**). In CA1, a significant increase in cleaved GSDMD-positive astrocytes was observed in the AD group (13.1 ± 4.1 cells/mm^2) compared to the non-AD group (0.4 ± 0.3 cells/mm^2, p = 0.0038) (**Fig. 2c**). Although in the temporal cortex a similar trend was observed for cleaved GSDMD-positive astrocytes in AD (12.6 ± 4 cells/mm^2) compared to non-AD cases (1.8 ± 0.8 cells/mm^2, p = 0.053), the difference did not reach statistical significance (**Fig. 2d**).

Since ASC and caspase-1, key players in canonical inflammasome activation, were not expressed in astrocytes, we analyzed the histological expression of caspase-8, a known inducer of the cleavage of GSDMD [10]. Interestingly, some astrocytes exhibited strong caspase-8 expression, predominantly in AD cases (**Fig. 3a-c**). Using immunofluorescence stainings, we detected co-expression of cleaved GSDMD and caspase-8 in GFAP-positive astrocytes (**Fig. 3d-g**). Finally, to exclude the involvement of caspase-8 in the extrinsic apoptosis pathway, we performed immunohistochemical stainings using an antibody for cleaved caspase-3, the apoptotic effector protein. Only physiological

expression of cleaved caspase-3 was observed in all groups (**Suppl. Fig. 3**), suggesting no execution of apoptosis.

Expression of cleaved GSDMD and non-canonical inflammasome protein caspase-4 in neurons of AD brain

Additional to microglia and astrocytes, also neurons in CA1 and temporal cortex were immunoreactive to cleaved GSDMD (**Fig. 4**). Predominantly in cases affected by AD pathology, expression of cleaved GSDMD was observed in the cytoplasm of pyramidal neurons. Sparse neurons in CA1 and the temporal cortex, mainly in layer III, were marked by strong expression of cleaved GSDMD, and showed shrinkage of the nucleus (**Fig. 4a-f**). NLRP3 and IL-18 showed minor expression in the cytoplasm of neurons across all groups, whereas no expression of ASC and caspase-1 was observed **(Suppl. Fig. 4)**.

Neurons with strong cytoplasmic immunoreactivity to cleaved GSDMD and shrunken nuclei, presumably undergoing pyroptosis (**Suppl. Fig. 1c**) were found in CA1 of 15 (out of 23) AD, 8 (out of 25) p-preAD and 2 (out of 22) non-AD cases. In the temporal cortex, these neurons were observed in 9 AD, 5 p-preAD and 1 non-AD cases. Overall, the number of cleaved GSDMD-positive neurons showing shrunken nuclei was low, and the differences between AD (1 ± 0.2 cells/mm^2), p-preAD (0.4 ± 0.1 cells/mm^2, p = 0.0214) and non-AD cases (0.2 ± 0.1 cells/mm^2, p = 0.0003) were minimal but significant (**Fig. 4g**). A similar trend was observed in layer III of the temporal cortex, where the number of cleaved GSDMD-positive neurons was increased in the AD group (0.9 ± 0.3 cells/mm^2) compared to the non-AD group (0.1 ± 0.1 cells/mm^2, p = 0.0101) (**Fig. 4h**). Expression of cleaved GSDMD was not observed in microglial cells or astrocytes interacting with or in close proximity to cleaved GSDMD-positive neurons.

Overall, pyramidal CA1 neurons showed physiological expression of caspase-8 in the cytoplasm (**Fig. 3a-c)**. However, some neurons in AD cases showed a more intense, granular immunostaining pattern for caspase-8 (**Fig. 3c).** Since expression of canonical inflammasome components ASC and

caspase-1 was not observed in neurons, and caspase-8 was not detected in cleaved GSDMD-positive neurons (**Fig. 5a**), we additionally analyzed the expression of caspase-4, a key player in the non-canonical inflammasome pathway [27]. We observed expression of caspase-4 in some cleaved GSDMD-positive neurons. Interestingly, neurons strongly immunoreactive to cleaved GSDMD were devoid of pTau-positive material (**Fig. 5c**). In line with this, pTau-filled neurons did not exhibit cleaved GSDMD (**Fig. 5d**). Likewise, expression of the necroptotic cell death effector pMLKL was not observed in cleaved GSDMD-positive neurons (**Suppl. Fig. 5a**). Vice versa, pMLKL-positive neurons did not express cleaved GSDMD (**Suppl. Fig. 5b**).

Expression of cleaved GSDMD in Aβ plaque-associated microglial cells and astrocytes

After delineating the cell type-specific expression of the NLRP3 inflammasome and pyroptosis-related proteins, we investigated the expression of the pyroptotic effector cleaved GSDMD in Aβ plaque-associated microglial cells and astrocytes. IBA1-positive microglial cells and GFAP-positive astrocytes marked by expression of cleaved GSDMD were observed in Aβ plaques in CA1 and the temporal cortex (**Fig. 6**). In addition, plaque-associated microglial cells also exhibited all NLRP3 inflammasome-forming proteins (NLRP3, ASC, caspase 1) and IL-18 (**Suppl. Fig. 4**). Correlation analysis showed moderate association of the number of cleaved GSDMD-positive cells and NLRP3-positive microglial cells, with parameters for AD pathology, e.g. AβMTL phase, Braak NFT stage, CERAD score and NIA-AA score, as well as the pMLKL-GVD stage (**Suppl. Table 3 a** and **b**). Notably, the number of cleaved GSDMD-positive microglial cells in CA1 correlated with abovementioned parameters, while this was not the case for the temporal cortex. Overall, the number of cleaved GSDMD-positive cells and microglia immunoreactive to the NLRP3 inflammasome-forming proteins, and IL-18, increased with increasing AβMTL phase and Braak NFT stage (**Suppl. Fig. 6-9**).

NLRP3-positive microglia and cleaved GSDMD-positive neurons associate with neuronal loss in CA1 of the hippocampus

To investigate the association between the expression of pyroptotic effector cleaved GSDMD and neuronal loss in AD, neuronal count per surface area (mm²) was used as a surrogate parameter for local neuronal loss. As our group previously reported [30], neuronal counts showed significant neuronal loss in the CA1 region of p-preAD (108.3 ± 3.0 cells/mm^2) compared to non-AD cases (131.9 ± 4.7 cells/mm^2, p = 0.0010), as well as in AD cases (80.9 ± 5.5 cells/mm^2) compared to both p-preAD (p = 0.0001) and non-AD cases (p < 0.0001) (**Suppl. Fig 10**). An additional analysis was performed to investigate the neuronal density in layer III of the temporal cortex. A significant decrease in the number of neurons per surface area was observed in the AD group (64.5 ± 2.5 cells/mm^2) compared to the non-AD control (77.3 ± 2.7 cells/mm^2, p = 0.0037) and p-preAD group (74.4 ± 2.4 cells/mm^2, p = 0.0474) (**Suppl. Fig 10**). No significant differences were observed between non-AD controls and p-preAD cases in the temporal cortex (p > 0.9999).

Next, we investigated a potential correlation of decreased neuronal density in CA1 or layer III of the temporal cortex, with the expression of the NLRP3 inflammasome and pyroptosis-related proteins. Correlation coefficient values between 0.3 and 0.7 were considered as moderate [39] and thus relevant correlations. A moderate negative correlation was found between the neuronal density in CA1 and the number of NLRP3-positive microglial cells (r = -0.481, p < 0.001), as well as with the number of cleaved GSDMD-positive neurons (r = -0.363, p = 0.002) in CA1 (**Suppl. Table 3**). Starting from a linear regression model including age and sex (RMSE = 26.91, R^2 = 0.30), hierarchical linear regression was performed using the highest correlating parameters, predicting the neuronal density in CA1 (**Suppl. Table 4**). The regression model including NLRP3-positive microglial cells (b = -1.557, p = < 0.001) and cleaved GSDMD-positive neurons (b = -11.06, p = 0.003) as predictor variables showed the lowest RMSE value (22.86) and highest R^2 (0.49) compared to other models (**Suppl. Table 5**). A combination of the latter two parameters could thus best predict the neuronal density in CA1 compared to regression models using other predictor variables. A similar analysis was performed in layer III of the temporal cortex. A weak negative correlation was found between the neuronal density in layer III of the temporal cortex and the number of caspase-1-positive microglial cells (r = -0.299, p =

0.013) (**Suppl. Table 4**). Starting from a linear regression model including the parameters age and sex (RMSE = 13.09, R^2 = 0.13), the addition of the predictor variable caspase-1-positive microglial cells (b = -1.254, *p* = 0.013) could best predict the neuronal density in layer III of the temporal cortex (RMSE = 12.68, R^2 = 0.18) compared to other predictor variables (**Suppl. Table 4**).

DISCUSSION

Here, we showed the presence of pyroptotic effector cleaved GSDMD in microglia, astrocytes and neurons of the MTL of symptomatic AD, p-preAD and non-AD control cases. Of these cell types, only microglia expressed all proteins forming the canonical NLRP3 inflammasome. Cleaved GSDMD-positive astrocytes of the AD-affected MTL were marked by the expression of caspase-8, while some cleaved GSDMD-positive neurons were marked by strong expression of caspase-4, also known as the non-canonical inflammasome [27]. Microglia and astrocytes positive for cleaved GSDMD were pronounced in close proximity to Aβ plaques although low levels of microglial cells and astrocytes were also found in the absence of Aβ plaques in the non-demented control cases. Cleaved GSDMD-positive neurons did not show pTau pathology and pTau-filled neurons did not express cleaved GSDMD. Finally, we showed that NLRP3-positive microglial cells and cleaved GSDMD-positive neurons moderately correlated inversely with the neuronal density in CA1. Collectively, we showed expression of all NLRP3 inflammasome-forming proteins, together with expression of cleaved GSDMD, in microglia, while astrocytes and neurons exhibited cleaved GSDMD in the absence of the NLRP3 inflammasome, pointing to alternative pyroptosis activation pathways via caspases 8 or 4 respectively. Thus, cell type-specific inflammasome and pyroptosis activation is part of the AD pathophysiology and may contribute to the neurodegenerative process (**Fig. 7**).

In the present study, we observed expression of the proteins forming the NLRP3 inflammasome, i.e. ASC, NLRP3 and caspase-1, as well as the pyroptosis-effector cleaved GSDMD, and IL-18, in microglia. These findings are in line with previous reports of NLRP3 inflammasome activation

in microglia, *in vitro*, in mouse models of AD pathology and multiple sclerosis (MS), and in patients with amyotrophic lateral sclerosis (ALS) [15, 19, 35, 46]. The presence of abundant ASC-positive microglial cells in all groups suggests physiological expression of this protein, while increased NLRP3- and cleaved GSDMD-positive microglial cells in CA1 and the temporal cortex of AD brain point to upregulation of NLRP3 and increased cleavage of GSDMD as a response to AD pathology. In both CA1 and the temporal cortex, some astrocytes and sparse pyramidal neurons exhibited NLRP3 and cleaved GSDMD, but lacked detectable amounts of ASC and caspase-1. Expression of IL-18 was also observed in some neurons. Although *in vitro* studies have reported NLRP3 inflammasome activation in astrocytes [22] and neurons [16], we did not observe expression of ASC and caspase-1 in these cell types in human brain samples. Recently, the expression of full length GSDMD was reported in oligodendrocytes of the AD-affected brain cortex [67]. However, we did not further investigate the expression of cleaved GSDMD in this cell type based on the lack of histopathological evidence of oligodendroglial cleaved GSDMD found in our samples. A recent study on pyroptosis in ALS reported microglial expression of cleaved GSDMD human ALS motor cortex and spinal cord [46], but no upregulation of cleaved GSDMD in neurons or astrocytes as seen here in AD. Thus, increased numbers of cleaved GSDMD-positive astrocytes and neurons seem to distinguish the pyroptosis activation pattern between AD and ALS.

The expression of all NLRP3 inflammasome proteins, cleaved GSDMD and IL-18 in microglia suggests NLRP3 inflammasome-mediated activation of pyroptosis in microglia in AD. The absence of ASC and caspase-1, key proteins for NLRP3 inflammasome formation, in astrocytes and neurons, suggests that these cell types do not undergo NLRP3 inflammasome-mediated activation of pyroptosis in AD. Although several other canonical inflammasomes have been described, of which some reported to function without ASC [31], the absence of caspase-1 argues against canonical inflammasome activation in astrocytes and neurons in AD. Interestingly, we observed expression of caspase-8, a known inducer of the cleavage of GSDMD [43], in the cytoplasm of hypertrophic astrocytes in cases affected by AD pathology, in line with an earlier study [41]. Although caspase-8 is also a molecular player in the extrinsic apoptosis pathway [6], the observed physiological expression of apoptotic

effector cleaved caspase-3 (**Suppl. Fig. 5**) seems to exclude activation of apoptosis. Finally, the observed upregulation of caspase-4 expression in cleaved GSDMD-positive neurons potentially indicates non-canonical inflammasome-mediated cleavage of GSDMD and thus pyroptosis activation. This is in line with earlier reports of caspase-4 being involved in AD pathogenesis, as well as endoplasmic reticulum (ER) stress- and Aβ-induced cell death [21, 26, 37].

Cleavage of GSDMD is followed by oligomerization of GSDMD-NT and formation of pores in the cell membrane, leading to cell death [44]. However, GSDMD pore formation can be regulated and does not inevitably lead to pyroptotic cell death [64]. Negative regulation of pyroptosis by the endosomal sorting complexes required for transport (ESCRT) machinery suggests a role for ESCRT-dependent plasma membrane repair in the removal of GSDMD pores, restricting pyroptotic cell death while favoring GSDMD-dependent cytokine release [42]. The observed granular immunostaining pattern of cleaved GSDMD, specifically in microglia, might indicate GSDMD-NT oligomerization. Together with the relatively high number of cleaved GSDMD-positive microglial cells, this potentially indicates restricted formation of GSDMD pores in the plasma membrane, without execution of pyroptotic cell death in most microglia. However, it is possible that some of these cleaved GSDMD-positive microglial cells eventually go into pyroptotic cell death, as previously suggested by Friker *et al* [9]. Similar mechanisms might be at play for cleaved GSDMD-positive astrocytes and neurons. Execution of pyroptotic cell death has been reported to occur as fast as within 45 min *in vitro* [60], making the observation of cells undergoing pyroptotic cell death in end-point post-mortem studies challenging. The sparse observation of cleaved GSDMD-positive neurons with shrunken nucleus, presumably undergoing pyroptosis, is expected considering the fast execution of pyroptotic cell death and long disease course of AD.

It is important to mention however, that the involvement of other cell death mechanisms such as apoptosis, necroptosis, ferroptosis, and autophagy-related cell death in AD pathogenesis is possible [8]. Although previous studies have reported execution of apoptosis in AD, these lack convincing evidence for the presence of neurons with apoptotic morphology and the expression of active caspase-

3 in brains with AD pathology [41, 53, 56], consistent with our histological observations for the expression of cleaved caspase-3. Activation of the necroptotic cell death mechanism in AD has recently been reported [5, 30], among which a previous study showing necroptosis activation in neurons of AD brain and specifically presence of necroptosis-related proteins within the vacuoles of GVD, as well as strong association with neuron loss [30]. Notably, caspase-8 has been suggested as a molecular switch between pyroptosis, apoptosis and the necroptotic cell death mechanism, activating the inflammasome and inducing pyroptosis when apoptosis and necroptosis cannot be executed [10]. This is in line with our observation of the absence of the necroptosis effector pMLKL in cleaved GSDMD-positive neurons, suggesting that activation of necroptosis and pyroptosis occur in distinct pyramidal neurons in AD. Although intracellular pTau pathology is thought to be the trigger for GVD [29, 62] and is associated with necroptosis activation in AD [5, 30], neuroinflammation as a result of pyroptosis activation could contribute to necroptosis activation as an additional stressor. This hypothesis is in line with the observed correlation of the number of NLRP3- and cleaved GSDMD-positive microglial cells, cleaved GSDMD-positive astrocytes and neurons, with the pMLKL-GVD stage (**Suppl. Table 3**).

Microglial cells and astrocytes immunoreactive to cleaved GSDMD accumulated around Aβ plaques, while the expression of cleaved GSDMD was not observed in neurons in the vicinity of Aβ plaques or in cells with pTau pathology. Considering the sensor protein NLRP3 is able to detect Aβ [15], these findings may point to Aβ as potential trigger for NLRP3 inflammasome-mediated activation of pyroptosis in Aβ plaque-associated microglial cells in AD. Given that cytokine release is known to impair the clearance of Aβ plaques by microglia [9, 19], the activation of the NLRP3 inflammasome and pyroptosis pathway, and subsequent cytokine release, might aggravate Aβ plaque deposition and contribute to the progression of Aβ pathology. Additionally, Aβ has been shown to interact with ASC released by pyroptotic cells, resulting in increased activation of the NLRP3 inflammasome and subsequent pyroptotic cell death [9], suggesting a vicious cycle of aggravating Aβ pathology and pro-inflammatory events. Moreover, IL-1β and IL-18 trigger signaling pathways that further enhance the inflammatory responses and create cytotoxic conditions leading to neuronal injury and death [51].

Collectively, these findings are in line with Aβ pathology driving an inflammatory response exacerbating over time [50]. This hypothesis is in accordance with our results showing correlation between the number of NLRP3- and cleaved GSDMD-positive microglial cells, cleaved GSDMD-positive astrocytes and neurons, and AβMTL phase (**Suppl. Table 3**). Since we did not observe presence of pTau pathology in cleaved GSDMD-positive neurons, the observed correlations of the number of NLRP3- and cleaved GSDMD-positive microglial cells, cleaved GSDMD-positive astrocytes and neurons with Braak NFT stage potentially represent indirect associations rather than direct, contributing to the development and propagation of pTau pathology possibly by cell lysis or Aβ-driven effects [12, 13, 33]. This is in line with an earlier study showing Aβ-induced Tau pathology via activation of the NLRP3 inflammasome [25]. However, evidence also exists for pathological Tau as a direct trigger of NLRP3 inflammasome activation [54]. Other damage-associated molecular patterns (DAMPs) such as reactive oxygen species (ROS) could be the trigger for caspase-4-mediated cleavage of GSDMD and neuronal pyroptosis activation. Our findings of cleaved GSDMD-positive astrocytes accumulating around Aβ plaques might indicate Aβ as a trigger for caspase-8-mediated cleavage of GSDMD and astrocytic pyroptosis activation, similar to our observations for the microglia.

In this study, we used neuronal counts per surface area (mm^2) as a surrogate parameter to investigate local neuronal loss and found increased neuronal loss in CA1, as previously reported [30], and increased neuronal loss in the temporal cortex, of AD cases. Overall, quantification of cells positive for cleaved GSDMD and the proteins of the NLRP3 inflammasome suggests the strongest NLRP3 inflammasome and pyroptosis activation in CA1. Moreover, the number of NLRP3-positive microglial cells and cleaved GSDMD-positive neurons were moderately associated with decreased neuronal density in CA1, suggesting that the activation of the NLRP3 inflammasome and pyroptosis contributes to neuronal loss in AD. In the temporal cortex, NLRP3 inflammasome and pyroptosis activation was less pronounced, as well as the correlation with the decreased neuronal density in this region. Taken together, our results suggest regional selectivity in the activation of the NLRP3 inflammasome and

pyroptosis in the AD-affected MTL with CA1 being more vulnerable than the temporal neocortex of Brodmann area 36.

Our findings showing activation of pyroptosis in AD and its potential cell type-specific pathways may have impact on the treatment of patients. First, our findings confirm earlier studies that the NLRP3 inflammasome is a potential target to lower the inflammatory reaction and damage in the brain [9, 19, 25, 61]. Second, we extend the current knowledge by showing that pyroptosis activation occurs in AD and may represent a novel therapeutic target to reduce neuroinflammatory brain damage. Finally, we show that not only microglial cells participate in inflammasome and pyroptosis activation, but also astrocytes and neurons, possibly via caspases 8 and 4, respectively. The cell type-specific variation of pyroptosis activation highlights the complexity of the neuroinflammatory response in AD. Distinct pathways may contribute to the neuroinflammatory response and neurodegeneration in AD. Accordingly, inhibiting NLRP3 inflammasome activation may not be enough to sufficiently reduce neuroinflammation and AD-related neuronal loss.

It has to be noted that comorbidity, agonal conditions and PMI may influence inflammatory responses in the brain, possibly influencing the quantified variables in this study. Comorbidity and agonal conditions were taken into account in the selection criteria of cases as much as possible. To control for the effect of the PMI, we included the PMI in the correlation analysis (**Suppl. Table 3** and **Suppl. Table 4**), showing no significant association with any of the investigated parameters. By using an antibody panel targeting the inflammasome as well as pyroptosis pathways, we provide ample evidence for inflammasome-mediated pyroptosis activation in AD. However, the immunohistochemical stainings for IL-18 and caspase-1 have to be interpreted with caution, since the used antibodies are reactive to the full length, but also cleaved forms of the proteins. Another inherent limitation of the analysis of human brain tissue is the lack of mechanistic understanding of the critical pathways. We can only provide association data which require functional validation in future *in vitro* and *in vivo* studies.

In conclusion, we show differential activation of inflammatory pathways, i.e. inflammasome and pyroptosis activation, in microglia, astrocytes and neurons in AD. This study provides new insights into inflammasome and pyroptosis activation in different cell types in the brain in response to AD pathology, potentially contributing to AD-related neuronal loss. It is essential to be aware of the complexity and variability of the neuroinflammatory response in AD in order to develop effective therapeutic strategies for AD patients.

Acknowledgements

This study was supported by funding from FWO-Vlaanderen (G0F8516N and G065721N, DRT). SM received a Doctoral mandate from KU Leuven internal funds (DB/20/007/BM). An SB PhD Fellowship from FWO-Vlaanderen was given to EVS (1S46219N). JMS is a junior postdoctoral fellow of the FWO-Vlaanderen (12Y1620N). We gratefully acknowledge the support of Ms. Simona Ospitalieri and Mrs. Alicja Ronisz, and the VIB Bio Imaging Core for their support & assistance in this study.

Author contributions

SM: study design, neuropathology, immunohistochemistry, microscopic assessments, statistical analysis, manuscript drafting and preparation. MK: study design, immunohistochemistry, microscopic assessments, critical review of the manuscript. EVS: immunohistochemistry, critical review of the manuscript. JMS: statistical analysis, critical review of the manuscript. RV, CAFvA: clinical neurology. TT: neuropathology and critical review of the manuscript. BDS: study design, critical review of the manuscript. DRT: study design and coordination, neuropathology, microscopic assessments and manuscript preparation. All authors read and approved the final manuscript.

Disclosures/Conflict of Interest

DRT is a member of the Acta Neuropathologica Editorial Board. He was not involved in the assessment or decision-making process for this manuscript. DRT received speaker honorary or travel

reimbursement from Novartis Pharma AG (Basel, Switzerland), UCB (Brussels, Belgium) and GE Healthcare (Amersham, UK), and collaborated with Novartis Pharma AG (Basel, Switzerland), Probiodrug (Halle (Saale), Germany), GE Healthcare (Amersham, UK), and Janssen Pharmaceutical Companies (Beerse, Belgium). Funders were not involved in the design of this study, in the collection, analysis or interpretation of data, in the decision to publish the results, or in the preparation of the manuscript.

FIGURES

Fig. 1 Histological expression of NLRP3-inflammasome and pyroptosis-related proteins in microglia in CA1 of AD brain. **a** Images of DAB stainings of the CA1 hippocampal region of representative symptomatic AD cases showing microglial cells immunoreactive to ASC, NLRP3, caspase-1, cleaved GSDMD and IL-18. High magnification images are shown on the right. **b** Images of immunofluorescence stainings of CA1 from representative symptomatic AD cases showing the expression of ASC, NLRP3, caspase-1, cleaved GSDMD, and IL-18 (red) in IBA1-positive microglia (green). Merged images are shown on the right. Scale bars represent 15 µm. **c**-**d** Quantification of cleaved GSDMD-positive microglial cells normalized to area (mm^2) in CA1 (**c**) and temporal cortex (layer I-VI) (**d**). The Kruskal-Wallis test was performed followed by Dunn's multiple comparisons test. Data is presented as mean with SEM. *Mi* immunoreactive microglia, Cl GSDMD *cleaved GSDMD, non-AD* non-demented control, *p-preAD* pathologically defined preclinical AD, *AD* symptomatic AD.

Fig. 2 NLRP3 and cleaved GSDMD, but not ASC, caspase-1 or IL-18 are expressed in astrocytes in CA1 of AD brain. **a** Images of DAB stainings of the CA1 hippocampal region of representative symptomatic AD cases showing astrocytes immunoreactive to NLRP3 and cleaved GSDMD, but not ASC, caspase-1 or IL-18. High magnification images are shown on the right. **b** Images of immunofluorescence stainings of CA1 from representative symptomatic AD cases showing the expression of NLRP3 and cleaved GSDMD, but not ASC, caspase-1 or IL-18 (red) in GFAP-positive astrocytes (green). Merged images are shown on the right. Scale bars represent 15 µm. **c**-**d** Quantification of cleaved GSDMD-positive

astrocytes normalized to area (mm²) in CA1 (**c**) and temporal cortex (layer I-VI) (**d**). The Kruskal-Wallis test was performed followed by Dunn's multiple comparisons test. Data is presented as mean with SEM. *As* immunoreactive astrocyte, *Mi* immunoreactive microglia, Cl GSDMD *cleaved GSDMD, non-AD* non-demented control, *p-preAD* pathologically defined preclinical AD, *AD* symptomatic AD.

Fig. 3 Caspase-8 is expressed in cleaved GSDMD-positive astrocytes in CA1 of AD brain. **a**-**c** Images of DAB stainings of the CA1 hippocampal region of representative non-AD, p-preAD and symptomatic AD cases using an antibody specific for caspase-8. Asterisk indicates a neuron with caspase 8-positive granules in the cytoplasm. **d**-**g** Images of immunofluorescence stainings of CA1 from a representative symptomatic AD case using antibodies specific for cleaved GSDMD (red), caspase-8 (green) and GFAP (cyan). Merged image is shown on the right. Scale bars represent 15 µm. *As* immunoreactive astrocyte, Cl GSDMD *cleaved GSDMD, non-AD* non-demented control, *p-preAD* pathologically defined preclinical AD, *AD* symptomatic AD.

Fig. 4 Cleaved GSDMD is expressed in pyramidal neurons of CA1 affected by AD pathology, of which sparse neurons are strongly immunoreactive. **a**-**c** Images of DAB stainings of the CA1 hippocampal region of representative non-AD, p-preAD and AD cases using an antibody specific for cleaved GSDMD. High magnification images are shown below (**d**-**f**). Scale bars represent 15 µm. **g**-**h** Quantification of neurons strongly immunoreactive to cleaved GSDMD with shrunken nuclei, normalized to area (mm²) in CA1 (**g**) and layer III of the temporal cortex (**h**). The Kruskal-Wallis test was performed followed by Dunn's multiple comparisons test. Data is presented as mean with SEM. Cl GSDMD *cleaved GSDMD, non-AD* non-demented control, *p-preAD* pathologically defined preclinical AD, *AD* symptomatic AD.

Fig. 5 Cleaved GSDMD-positive neurons exhibit caspase-4, but not caspase-8 or pTau pathology. Images of representative immunofluorescence stainings of CA1 from symptomatic AD cases showing absence of caspase-8 (green) (**a**) and expression of caspase-4 (green) (**b**) in a cleaved GSDMD-positive (red) pyramidal neuron. **c** Absence of NFT/pTau (AT8, cyan) in a cleaved GSDMD-positive (red) neuron. **d** absence of cleaved GSDMD in a pTau-filled neuron**.** DAPI (blue) was used to visualize nuclei. Full

arrows indicate cleaved GSDMD-positive only pyramidal neurons. White arrowheads indicate cleaved GSDMD-negative, caspase-8- or AT8-positive pyramidal neurons. Red arrowheads indicate a cleaved GSDMD-positive, caspase-4-positive pyramidal neuron. Scale bars represent 15 µm. Cl GSDMD *cleaved GSDMD, AD* symptomatic AD.

Fig. 6 Cleaved GSDMD is expressed in microglia and astrocytes in close proximity to Aβ plaques. **a**-**b** Images of representative immunofluorescence stainings of symptomatic AD temporal cortex using antibodies specific for cleaved GSDMD (red), IBA1 (green) (**a**) or GFAP (green) (**b**), and Aβ (4G8, cyan), with DAPI (blue) staining of nuclei. Arrowheads indicate expression of cleaved GSDMD in an IBA1+ microglial cell. Scale bars represent 15 µm. *Mi* microglia, *As* immunoreactive astrocyte, Cl GSDMD *cleaved GSDMD, AD* symptomatic AD.

Fig. 7 Cell type-specific pyroptosis activation in AD. In microglia, the canonical NLRP3 inflammasome is formed by the sensor protein NLRP3, the adaptor protein ASC and inflammatory caspase-1, as a result of emerging neuropathology. Activated caspase-1 p20 cleaves GSDMD and initiates pyroptosis activation, potentially leading to GSDMD-NT pore formation in the plasma membrane. In astrocytes, the observed expression of caspase-8 potentially indicates an alternative pathway for the cleavage of GSDMD and pyroptosis activation. Likewise, expression of caspase-4 in some cleaved GSDMD-positive pyramidal neurons could points to caspase-4-mediated cleavage of GSDMD. Inflammasome and pyroptosis activation is expected to increase with the progression of AD pathology. No or very few pyroptotic cells were observed in non-AD cases, while pyroptotic microglial cells, astrocytes and neurons were observed in p-preAD cases, with increased prevalence in AD cases.

REFERENCES

1. Arranz AM, De Strooper B (2019) The role of astroglia in Alzheimer's disease: pathophysiology and clinical implications. Lancet Neurol 18:406–414. doi: 10.1016/S1474-4422(18)30490-3

2. Braak H, Alafuzoff I, Arzberger T, Kretzschmar H, Tredici K (2006) Staging of Alzheimer disease-associated neurofibrillary pathology using paraffin sections and immunocytochemistry. Acta

Neuropathol 112:389–404. doi: 10.1007/s00401-006-0127-z

3. Braak H, Braak E (1991) Neuropathological stageing of Alzheimer-related changes. Acta Neuropathol 82:239–259. doi: 10.1007/bf00308809

4. Cacace R, Sleegers K, Broeckhoven C Van (2016) Molecular genetics of early-onset Alzheimer ' s disease revisited. Alzheimer's Dement 12:733–748. doi: 10.1016/j.jalz.2016.01.012

5. Caccamo A, Branca C, Piras IS, Ferreira E, Huentelman MJ, Liang WS, Readhead B, Dudley JT, Spangenberg EE, Green KN, Belfiore R, Winslow W, Oddo S (2017) Necroptosis activation in Alzheimer's disease. Nat Neurosci 20:1236–1246. doi: 10.1038/nn.4608

6. Cavalcante GC, Schaan AP, Cabral GF, Santana-Da-Silva MN, Pinto P, Vidal AF, Ribeiro-Dos-Santos Â (2019) A cell's fate: An overview of the molecular biology and genetics of apoptosis. Int J Mol Sci 20:1–20. doi: 10.3390/ijms20174133

7. Crary JF, Trojanowski JQ, Schneider JA, Abisambra JF, Abner EL, Alafuzoff I, Arnold SE, Attems J, Beach TG, Bigio EH, Cairns NJ, Dickson DW, Gearing M, Grinberg LT, Hof PR, Hyman BT, Jellinger K, Jicha GA, Kovacs GG, Knopman DS, Kofler J, Kukull WA, Mackenzie IR, Masliah E, McKee A, Montine TJ, Murray ME, Neltner JH, Santa-Maria I, Seeley WW, Serrano-Pozo A, Shelanski ML, Stein T, Takao M, Thal DR, Toledo JB, Troncoso JC, Vonsattel JP, White CL, Wisniewski T, Woltjer RL, Yamada M, Nelson PT (2014) Primary age-related tauopathy (PART): a common pathology associated with human aging. Acta Neuropathol 128:755–766. doi: 10.1007/s00401-014-1349-0

8. Fricker M, Tolkovsky AM, Borutaite V, Coleman M, Brown GC (2018) Neuronal cell death. Physiol Rev 98:813–880. doi: 10.1152/physrev.00011.2017

9. Friker LL, Scheiblich H, Hochheiser I V., Brinkschulte R, Riedel D, Latz E, Geyer M, Heneka MT (2020) β-Amyloid Clustering around ASC Fibrils Boosts Its Toxicity in Microglia. Cell Rep 30:3743–3754. doi: 10.1016/j.celrep.2020.02.025

10. Fritsch M, Günther SD, Schwarzer R, Albert MC, Schorn F, Werthenbach JP, Schiffmann LM, Stair N, Stocks H, Seeger JM, Lamkanfi M, Krönke M, Pasparakis M, Kashkar H (2019) Caspase-8 is the molecular switch for apoptosis, necroptosis and pyroptosis. Nature 575:683–687. doi: 10.1038/s41586-019-1770-6

11. García-Cabezas M, John YJ, Barbas H, Zikopoulos B (2016) Distinction of neurons, glia and endothelial cells in the cerebral cortex: An algorithm based on cytological features. Front Neuroanat 10:1–28. doi: 10.3389/fnana.2016.00107

12. Gomes LA, Hipp SA, Rijal Upadhaya A, Balakrishnan K, Ospitalieri S, Koper MJ, Largo-Barrientos P, Uytterhoeven V, Reichwald J, Rabe S, Vandenberghe R, von Arnim CAF, Tousseyn T, Feederle R, Giudici C, Willem M, Staufenbiel M, Thal DR (2019) Aβ-induced acceleration of Alzheimer-related τ-pathology spreading and its association with prion protein. Acta Neuropathol 138:913–941. doi: 10.1007/s00401-019-02053-5

13. Götz J, Chen F, Van Dorpe J, Nitsch RM (2001) Formation of neurofibrillary tangles in P301L tau transgenic mice induced by Aβ42 fibrils. Science 293:1491–1495. doi: 10.1126/science.1062097

14. Griffin WST, Sheng JG, Roberts GW, Mrak RE (1995) Interleukin-1 Expression in Different Plaque Types in Alzheimer's Disease. J. Neuropathol. Exp. Neurol. 54:276–281

15. Halle A, Hornung V, Petzold GC, Stewart CR, Monks BG, Reinheckel T, Fitzgerald KA, Latz E, Moore KJ, Golenbock DT (2008) The NALP3 inflammasome is involved in the innate immune response to amyloid-β. Nat Immunol 9:857–865. doi: 10.1038/ni.1636

16. Han C, Yang Y, Guan Q, Zhang X, Shen H, Sheng Y, Wang J, Zhou X, Li W, Guo L, Jiao Q (2020) New mechanism of nerve injury in Alzheimer's disease: β-amyloid-induced neuronal pyroptosis. J Cell Mol Med 24:8078–8090. doi: 10.1111/jcmm.15439

17. He W, Wan H, Hu L, Chen P, Wang X, Huang Z, Yang Z, Zhong C, Han J (2015) Gasdermin D is

an executor of pyroptosis and required for interleukin-1 β secretion. Cell Res 25:1285–1298. doi: 10.1038/cr.2015.139

18. Hecht M, Krämer LM, von Arnim CAF, Otto M, Thal DR (2018) Capillary cerebral amyloid angiopathy in Alzheimer's disease: association with allocortical/hippocampal microinfarcts and cognitive decline. Acta Neuropathol 135:681–694. doi: 10.1007/s00401-018-1834-y

19. Heneka MT, Kummer MP, Stutz A, Delekate A, Schwartz S, Vieira-Saecker A, Griep A, Axt D, Remus A, Tzeng TC, Gelpi E, Halle A, Korte M, Latz E, Golenbock DT (2013) NLRP3 is activated in Alzheimer's disease and contributes to pathology in APP/PS1 mice. Nature 493:674–678. doi: 10.1038/nature11729

20. Heneka MT, McManus RM, Latz E (2018) Inflammasome signalling in brain function and neurodegenerative disease. Nat Rev Neurosci 19:610–621. doi: 10.1038/s41583-018-0055-7

21. Hitomi J, Katayama T, Eguchi Y, Kudo T, Taniguchi M, Koyama Y, Manabe T, Yamagishi S, Bando Y, Imaizumi K, Tsujimoto Y, Tohyama M (2004) Involvement of caspase-4 in endoplasmic reticulum stress-induced apoptosis and Aβ-induced cell death. J Cell Biol 165:347–356. doi: 10.1083/jcb.200310015

22. Hong Y, Liu Y, Yu D, Wang M, Hou Y (2019) The neuroprotection of progesterone against Aβ-induced NLRP3-Caspase-1 inflammasome activation via enhancing autophagy in astrocytes. Int Immunopharmacol 74. doi: 10.1016/j.intimp.2019.05.054

23. Hughes CP, Berg L, Danziger WL, Coben LA, Martin RL (1982) A new clinical scale for the staging of dementia. Br J Psychiatry 140:566–572. doi: 10.1192/bjp.140.6.566

24. Hyman BT, Phelps CH, Beach TG, Bigio EH, Cairns NJ, Carrillo MC, Dickson DW, Duyckaerts C, Frosch MP, Masliah E, Mirra SS, Nelson PT, Schneider JA, Thal DR, Thies B, Trojanowski JQ, Vinters H V., Montine TJ (2012) National Institute on Aging-Alzheimer's Association guidelines for the neuropathologic assessment of Alzheimer's disease. Alzheimer's Dement 8:1–13. doi:

10.1016/j.jalz.2011.10.007

25. Ising C, Venegas C, Zhang S, Scheiblich H, Schmidt S V, Vieira-saecker A, Schwartz S, Albasset S, Mcmanus RM, Tejera D, Griep A, Santarelli F, Brosseron F, Opitz S, Stunden J, Merten M, Kayed R, Golenbock DT, Blum D, Latz E, Buée L, Heneka MT (2019) NLRP3 inflammasome activation drives tau pathology. Nature 575:669–673. doi: 10.1038/s41586-019-1769-z

26. Kajiwara Y, McKenzie A, Dorr N, Gama Sosa MA, Elder G, Schmeidler J, Dickstein DL, Bozdagi O, Zhang B, Buxbaum JD (2016) The human-specific CASP4 gene product contributes to Alzheimer-related synaptic and behavioural deficits. Hum Mol Genet 25:4315–4327. doi: 10.1093/hmg/ddw265

27. Kayagaki N, Warming S, Lamkanfi M, Walle L Vande, Louie S, Dong J, Newton K, Qu Y, Liu J, Heldens S, Zhang J, Lee WP, Roose-Girma M, Dixit VM (2011) Non-canonical inflammasome activation targets caspase-11. Nature 479:117–121. doi: 10.1038/nature10558

28. Kinney JW, Bemiller SM, Murtishaw AS, Leisgang AM, Salazar AM, Lamb BT (2018) Inflammation as a central mechanism in Alzheimer's disease. Alzheimer's Dement Transl Res Clin Interv 4:575–590. doi: 10.1016/j.trci.2018.06.014

29. Köhler C, Dinekov M, Götz J (2014) Granulovacuolar degeneration and unfolded protein response in mouse models of tauopathy and Aβ amyloidosis. Neurobiol Dis 71:169–179. doi: 10.1016/j.nbd.2014.07.006

30. Koper MJ, Van Schoor E, Ospitalieri S, Vandenberghe R, Vandenbulcke M, von Arnim CAF, Tousseyn T, Balusu S, De Strooper B, Thal DR (2020) Necrosome complex detected in granulovacuolar degeneration is associated with neuronal loss in Alzheimer's disease. Acta Neuropathol 139:463–484. doi: 10.1007/s00401-019-02103-y

31. Lamkanfi M, Dixit VM (2014) Mechanisms and functions of inflammasomes. Cell 157:1013–1022. doi: 10.1016/j.cell.2014.04.007

32. Latz E, Xiao TS, Stutz A (2013) Activation and regulation of the inflammasomes. Nat Rev Immunol 13:397–411. doi: 10.1038/nri3452

33. Lewis J, Dickson DW, Lin WL, Chisholm L, Corral A, Jones G, Yen SH, Sahara N, Skipper L, Yager D, Eckman C, Hardy J, Hutton M, McGowan E (2001) Enhanced neurofibrillary degeneration in transgenic mice expressing mutant tau and APP. Science 293:1487–1491. doi: 10.1126/science.1058189

34. Masters CL, Bateman R, Blennow K, Rowe CC, Sperling RA, Cummings JL (2015) Alzheimer's disease. Nat Rev Dis Prim 1:1–18. doi: 10.1038/nrdp.2015.56

35. McKenzie BA, Mamik MK, Saito LB, Boghozian R, Monaco MC, Major EO, Lu JQ, Branton WG, Power C (2019) Caspase-1 inhibition prevents glial inflammasome activation and pyroptosis in models of multiple sclerosis. Proc Natl Acad Sci U S A 116:13145. doi: 10.1073/pnas.1909025116

36. Mirra SS, Heyman A, McKeel D, Sumi SM, Crain BJ, Brownlee LM, Vogel FS, Hughes JP, van Belle G, Berg L (1991) The Consortium to Establish a Registry for Alzheimer's Disease (CERAD). Part II. Standardization of the neuropathologic assessment of Alzheimer's disease. Neurology 41:479–486. doi: 10.1212/wnl.41.4.479

37. Nishizaki T (2019) Fe 3 + Facilitates Endocytic Internalization of Extracellular A β 1 – 42 and Enhances A β 1 – 42 -Induced Caspase-3 / Caspase-4 Activation and Neuronal Cell Death. Mol Neurobiol 56:4812–4819. doi: https://doi.org/10.1007/s12035-018-1408-y

38. Ransohoff RM (2016) How neuroinflammation contributes to neurodegeneration. Science 353:777–783. doi: 10.1126/science.aag2590

39. Ratner B (2009) The correlation coefficient: Its values range between 1/1, or do they. J Targeting, Meas Anal Mark 17:139–142. doi: 10.1057/jt.2009.5

40. Rijal Upadhaya A, Kosterin I, Kumar S, Von Arnim CAF, Yamaguchi H, Fändrich M, Walter J,

Thal DR (2014) Biochemical stages of amyloid-β peptide aggregation and accumulation in the human brain and their association with symptomatic and pathologically preclinical Alzheimer's disease. Brain 137:887–903. doi: 10.1093/brain/awt362

41. Rohn TT, Head E, Nesse WH, Cotman CW, Cribbs DH (2001) Activation of caspase-8 in the Alzheimer's disease brain. Neurobiol Dis 8:1006–1016. doi: 10.1006/nbdi.2001.0449

42. Rühl S, Shkarina K, Demarco B, Heilig R, Santos JC, Broz P (2018) ESCRT-dependent membrane repair negatively regulates pyroptosis downstream of GSDMD activation. Science 362:956–960. doi: 10.1126/science.aar7607

43. Sarhan J, Liu BC, Muendlein HI, Li P, Nilson R, Tang AY, Rongvaux A, Bunnell SC, Shao F, Green DR, Poltorak A (2018) Caspase-8 induces cleavage of gasdermin D to elicit pyroptosis during Yersinia infection. Proc Natl Acad Sci U S A 115:E10888–E10897. doi: 10.1073/pnas.1809548115

44. Sborgi L, Rühl S, Mulvihill E, Pipercevic J, Heilig R, Stahlberg H, Farady CJ, Müller DJ, Broz P, Hiller S (2016) GSDMD membrane pore formation constitutes the mechanism of pyroptotic cell death . EMBO J 35:1766–1778. doi: 10.15252/embj.201694696

45. Schaeverbeke JM, Gabel S, Meersmans K, Luckett ES, De Meyer S, Adamczuk K, Nelissen N, Goovaerts V, Radwan A, Sunaert S, Dupont P, Van Laere K, Vandenberghe R (2021) Baseline cognition is the best predictor of 4-year cognitive change in cognitively intact older adults. Alzheimer's Res Ther 13:1–16. doi: 10.1186/s13195-021-00798-4

46. Van Schoor E, Ospitalieri S, Moonen S, Tomé SO, Ronisz A, Ok O, Dedeene L, Weishaupt J, Ludolph AC, van Damme P, Van Den Bosch L, Thal DR (2022) Increased pyroptosis activation in white matter microglia is associated with neuronal loss in ALS motor cortex. Acta Neuropathol

47. Serrano-pozo A, Mielke ML, Gómez-isla T, Betensky RA, Growdon JH, Frosch MP, Hyman BT (2011) Reactive Glia not only Associates with Plaques but also Parallels Tangles in Alzheimer '

s Disease. AJPA 179:1373–1384. doi: 10.1016/j.ajpath.2011.05.047

48. Shi J, Gao W, Shao F (2017) Pyroptosis: Gasdermin-Mediated Programmed Necrotic Cell Death. Trends Biochem Sci 42:245–254. doi: 10.1016/j.tibs.2016.10.004

49. Shi J, Zhao Y, Wang K, Shi X, Wang Y, Huang H, Zhuang Y, Cai T, Wang F, Shao F (2015) Cleavage of GSDMD by inflammatory caspases determines pyroptotic cell death. Nature 526:660–665. doi: 10.1038/nature15514

50. Sierksma A, Lu A, Mancuso R, Fattorelli N, Thrupp N, Salta E, Zoco J, Blum D, Buée L, De Strooper B, Fiers M (2020) Novel Alzheimer risk genes determine the microglia response to amyloid-β but not to TAU pathology. EMBO Mol Med 12:1–18. doi: 10.15252/emmm.201910606

51. Song L, Pei L, Yao S, Wu Y, Shang Y (2017) NLRP3 inflammasome in neurological diseases, from functions to therapies. Front Cell Neurosci 11:1–17. doi: 10.3389/fncel.2017.00063

52. Sperling RA, Aisen PS, Beckett LA, Bennett DA, Craft S, Fagan AM, Iwatsubo T, Jack CR, Kaye J, Montine TJ, Park DC, Reiman EM, Rowe CC, Siemers E, Stern Y, Yaffe K, Carrillo MC, Thies B, Morrison-Bogorad M, Wagster M V., Phelps CH (2011) Toward defining the preclinical stages of Alzheimer's disease: Recommendations from the National Institute on Aging-Alzheimer's Association workgroups on diagnostic guidelines for Alzheimer's disease. Alzheimer's Dement 7:280–292. doi: 10.1016/j.jalz.2011.03.003

53. Stadelmann C, Deckwerth TL, Srinivasan A, Bancher C, Brück W, Jellinger K, Lassmann H (1999) Activation of caspase-3 in single neurons and autophagic granules of granulovacuolar degeneration in Alzheimer's disease: Evidence for apoptotic cell death. Am J Pathol 155:1459–1466. doi: 10.1016/S0002-9440(10)65460-0

54. Stancu IC, Cremers N, Vanrusselt H, Couturier J, Vanoosthuyse A, Kessels S, Lodder C, Brône B, Huaux F, Octave JN, Terwel D, Dewachter I (2019) Aggregated Tau activates NLRP3–ASC

inflammasome exacerbating exogenously seeded and non-exogenously seeded Tau pathology in vivo. Acta Neuropathol 137:599–617. doi: 10.1007/s00401-018-01957-y

55. Stence N, Waite M, Dailey ME (2001) Dynamics of microglial activation: A confocal time-lapse analysis in hippocampal slices. Glia 33:256–266. doi: 10.1002/1098-1136(200103)33:3<256::AID-GLIA1024>3.0.CO;2-J

56. Su JH, Zhao M, Anderson AJ, Srinivasan A, Cotman CW (2001) Activated caspase-3 expression in Alzheimer's and aged control brain: Correlation with Alzheimer pathology. Brain Res 898:350–357. doi: 10.1016/S0006-8993(01)02018-2

57. Thal DR, Rüb U, Orantes M, Braak H (2002) Phases of Aβ-deposition in the human brain and its relevance for the development of AD. Neurology 58:1791–1800. doi: 10.1212/WNL.58.12.1791

58. Thal DR, Rüb U, Schultz C, Sassin I, Ghebremedhin E, Del Tredici K, Braak E, Braak H (2000) Sequence of Aβ-protein deposition in the human medial temporal lobe. J Neuropathol Exp Neurol 59:733–748. doi: 10.1093/jnen/59.8.733

59. Thal DR, Del Tredici K, Ludolph AC, Hoozemans JJM, Rozemuller AJ, Braak H, Knippschild U (2011) Stages of granulovacuolar degeneration: Their relation to Alzheimer's disease and chronic stress response. Acta Neuropathol 122:577–589. doi: 10.1007/s00401-011-0871-6

60. de Vasconcelos NM, Van Opdenbosch N, Van Gorp H, Parthoens E, Lamkanfi M (2019) Single-cell analysis of pyroptosis dynamics reveals conserved GSDMD-mediated subcellular events that precede plasma membrane rupture. Cell Death Differ 26:146–161. doi: 10.1038/s41418-018-0106-7

61. Venegas C, Kumar S, Franklin BS, Dierkes T, Brinkschulte R, Tejera D, Vieira-Saecker A, Schwartz S, Santarelli F, Kummer MP, Griep A, Gelpi E, Beilharz M, Riedel D, Golenbock DT, Geyer M, Walter J, Latz E, Heneka MT (2017) Microglia-derived ASC specks crossseed amyloid-

β in Alzheimer's disease. Nature 552:355–361. doi: 10.1038/nature25158

62. Wiersma VI, Ziel AM Van, Vazquez S, Anna S, Ernesto N, Correa B, Bonaterra A, Florence P, Markus C, René T, Jan JPM, Verhage M, Hoozemans JJM, Scheper W (2019) Granulovacuolar degeneration bodies are neuron-selective lysosomal structures induced by intracellular tau pathology. Acta Neuropathol 138:943–970. doi: 10.1007/s00401-019-02046-4

63. World Health Organization (2017) Global action plan on the public health response to dementia 2017 - 2025. http://www.who.int/mental_health/neurology/dementia/action_plan_2017_2025/en/

64. Zahid A, Ismail H, Jin T (2021) Molecular and structural aspects of gasdermin family pores and insights into gasdermin-elicited programmed cell death. Biochem Soc Trans 49:2697–2710. doi: 10.1042/BST20210672

65. Zarow C, Vinters H V., Ellis WG, Weiner MW, Mungas D, White L, Chui HC (2005) Correlates of hippocampal neuron number in Alzheimer's disease and ischemic vascular dementia. Ann Neurol 57:896–903. doi: 10.1002/ana.20503

66. Zendedel A, Johann S, Mehrabi S, Joghataei M taghi, Hassanzadeh G, Kipp M, Beyer C (2016) Activation and Regulation of NLRP3 Inflammasome by Intrathecal Application of SDF-1a in a Spinal Cord Injury Model. Mol Neurobiol 53:3063–3075. doi: 10.1007/s12035-015-9203-5

67. Zhang X, Wang R, Hu D, Sun X, Fujioka H, Lundberg K, Chan ER, Wang Q, Xu R, Flanagan ME, Pieper AA, Qi X (2020) Oligodendroglial glycolytic stress triggers inflammasome activation and neuropathology in Alzheimer's disease. Sci Adv 6. doi: 10.1126/sciadv.abb8680

Fig. 1 Histological expression of NLRP3 inflammasome and pyroptosis-related proteins in microglia of CA1 in AD brain.

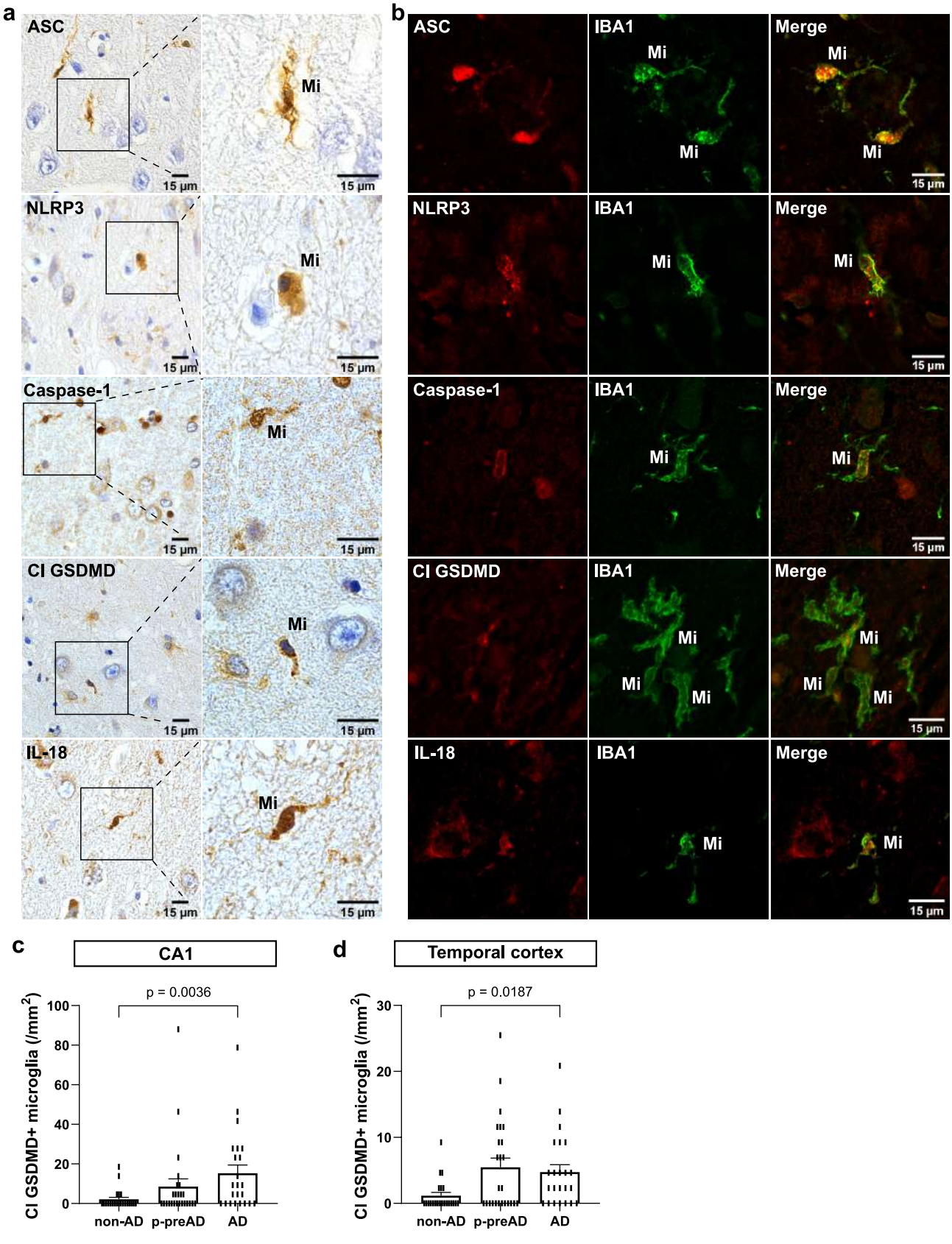

Fig. 2 NLRP3 and cleaved GSDMD, but not ASC, caspase-1 or IL-18 are expressed in astrocytes of CA1 in AD brain.

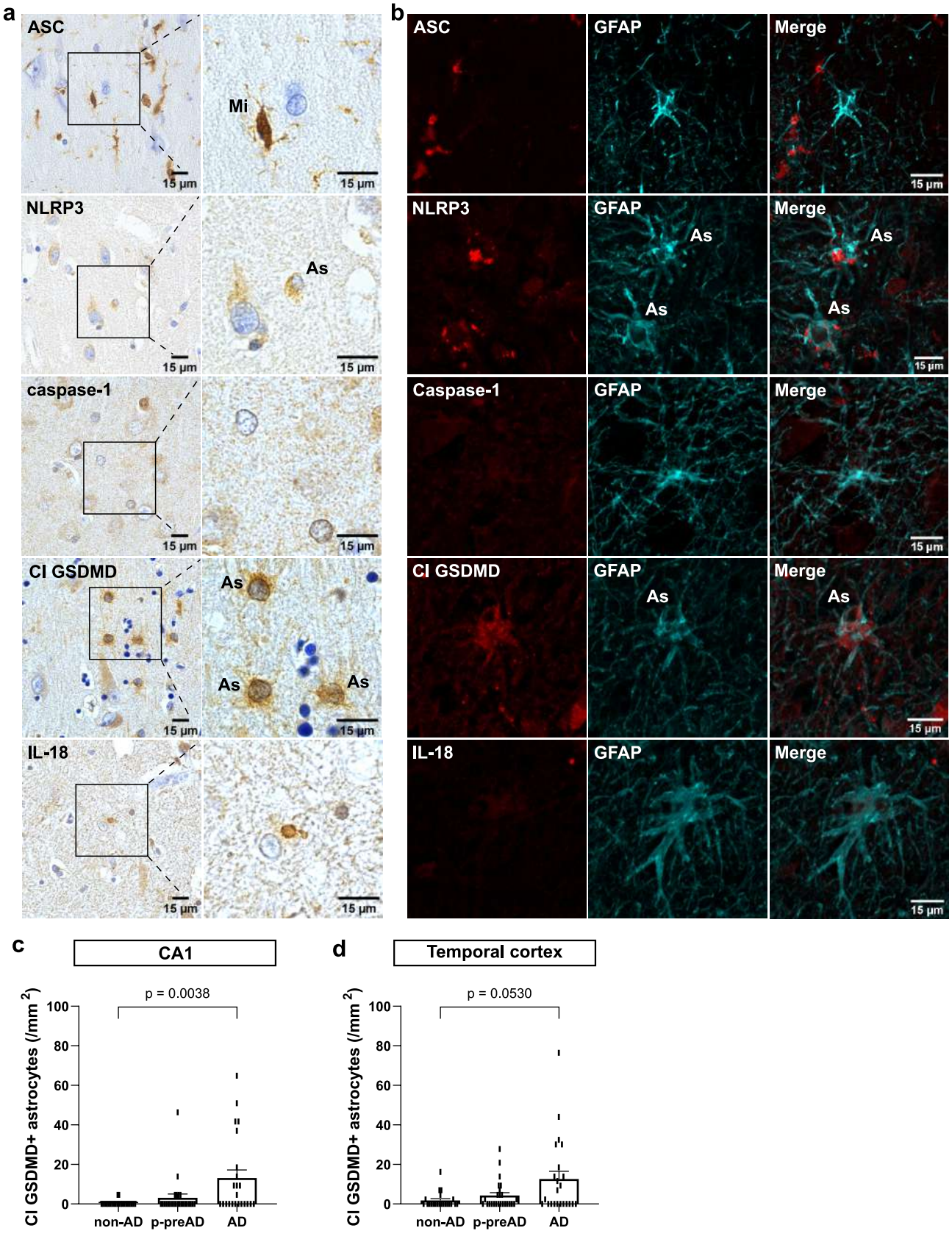

Fig. 3 Caspase-8 is expressed in cleaved GSDMD-positive astrocytes in CA1 of AD brain.

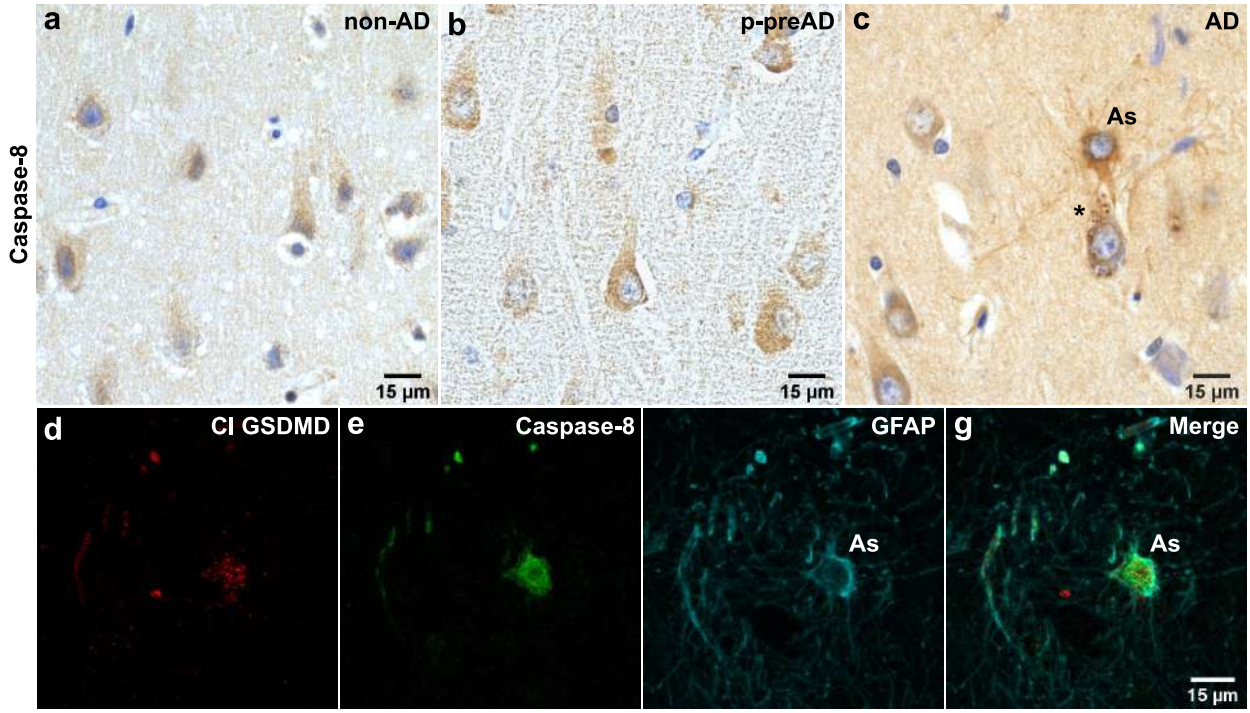

Fig. 4 Cleaved GSDMD is expressed in pyramidal neurons of CA1 affected by AD pathology, of which sparse neurons are strongly immunoreactive.

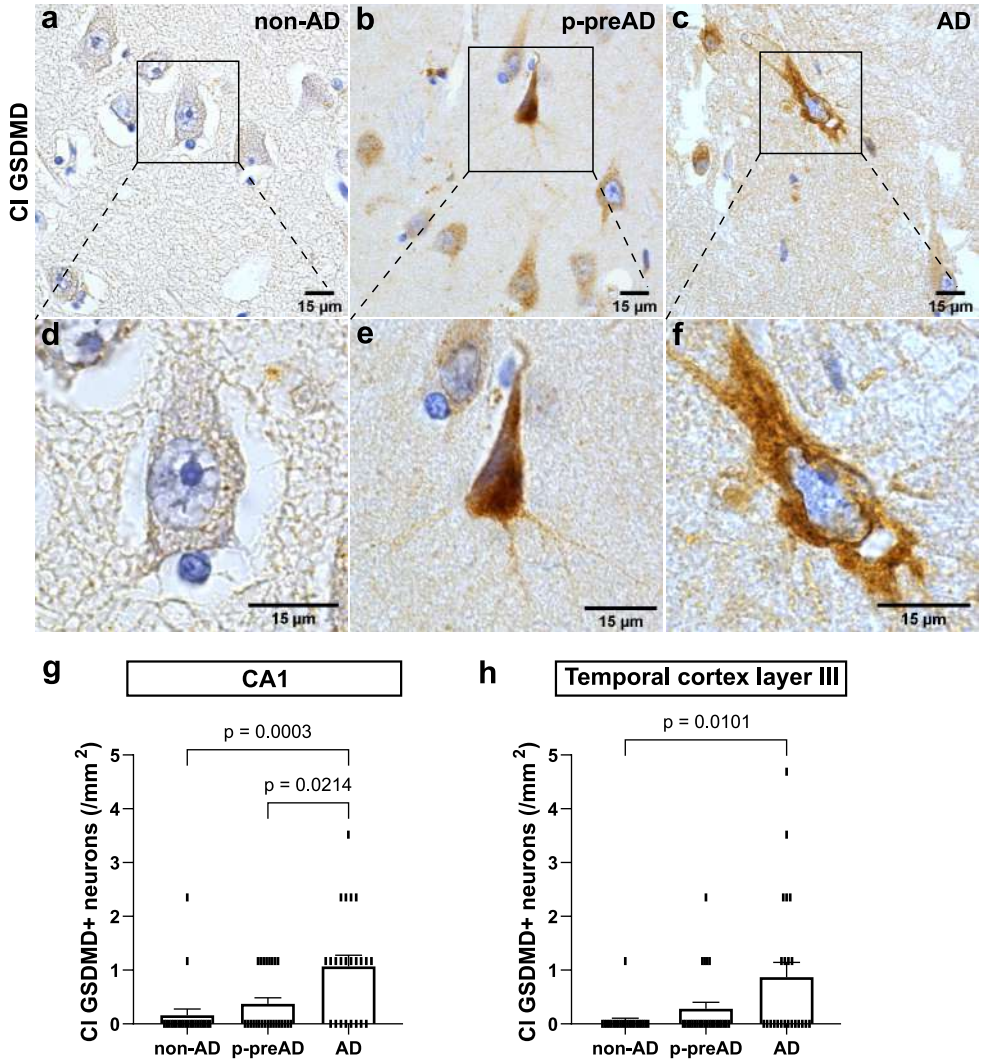

Fig. 5 Cleaved GSDMD-positive neurons exhibit caspase-4, but not caspase-8 or pTau pathology.

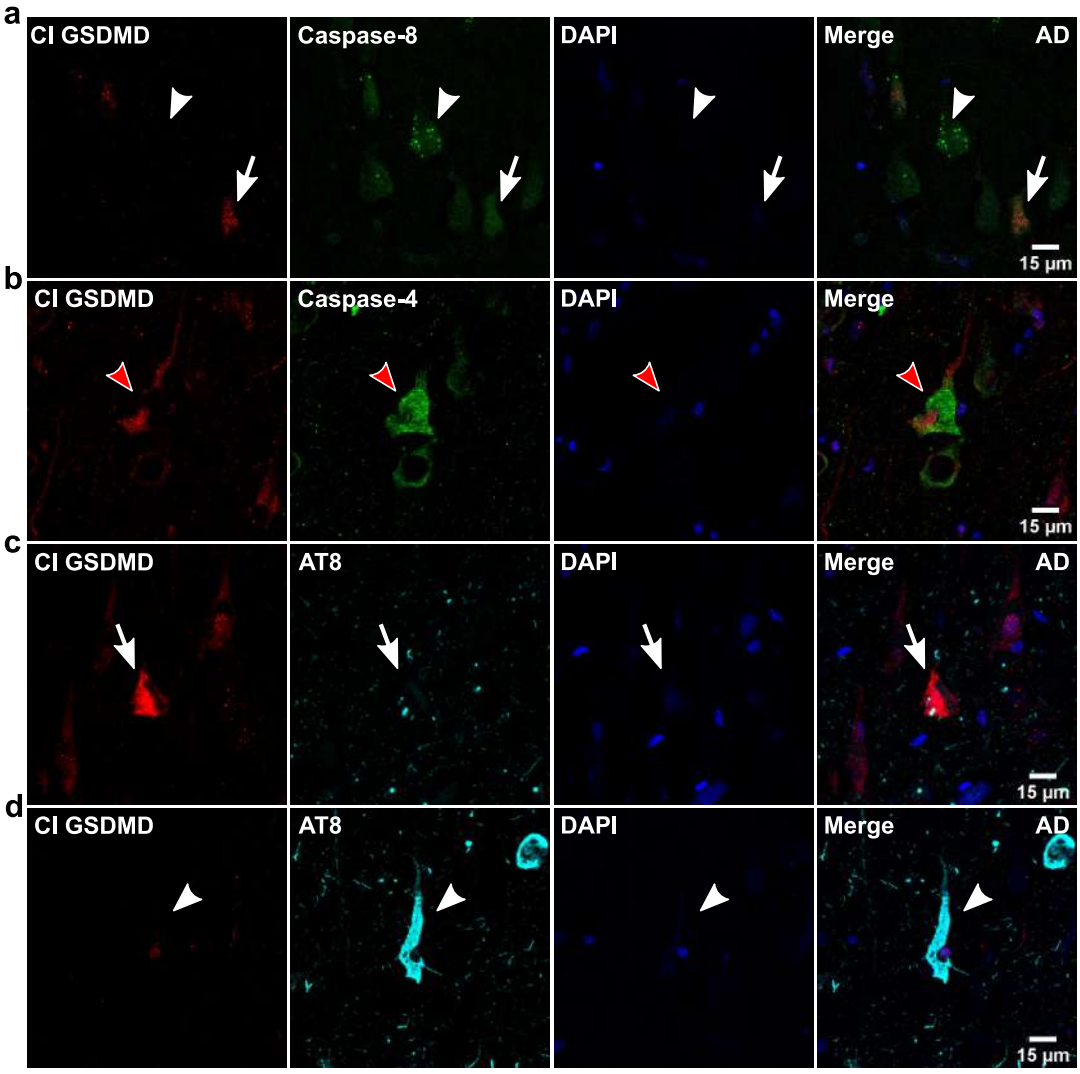

Fig. 6 Cleaved GSDMD is expressd in microglia and astrocytes in close proximity to Aβ plaques.

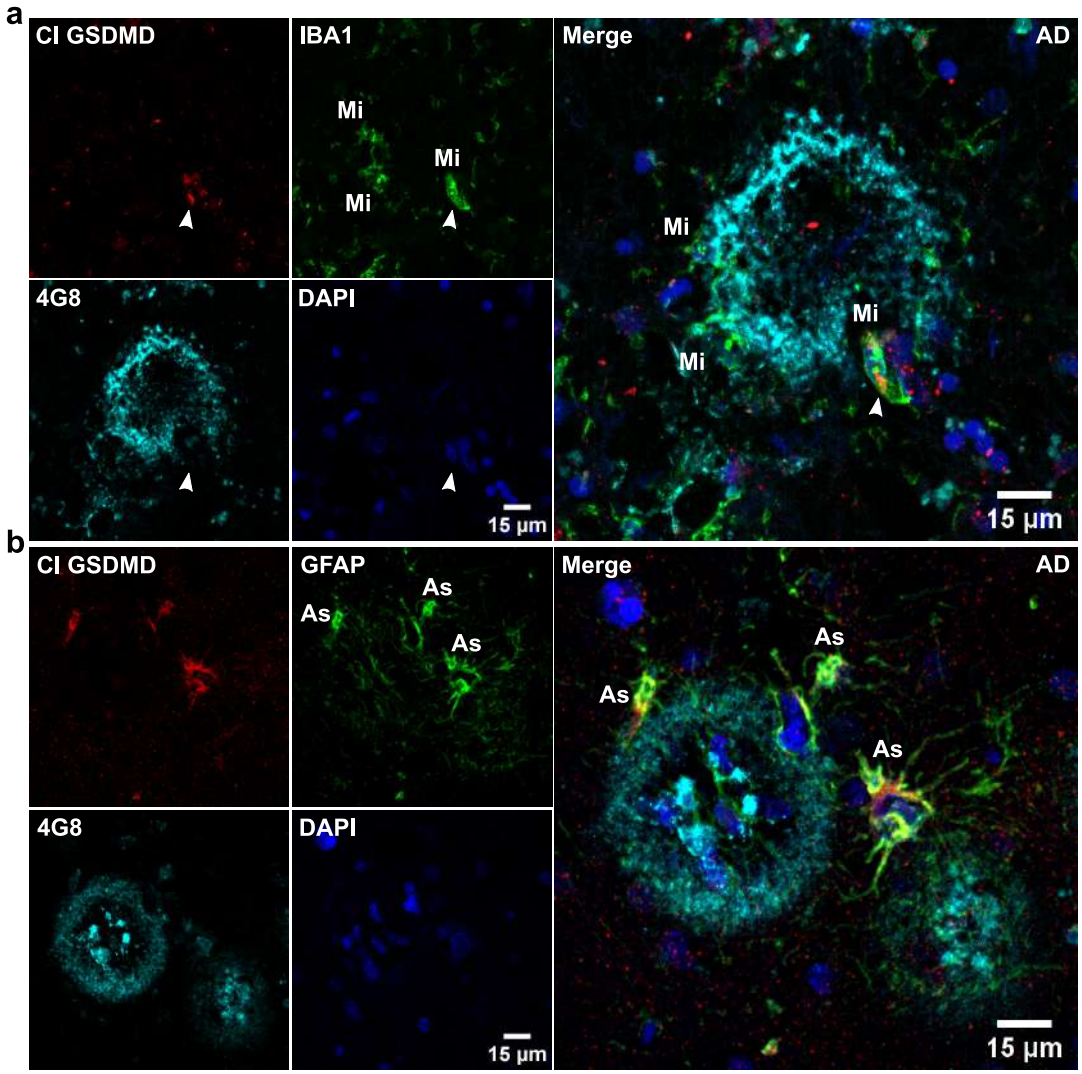

Fig. 7 Cell type-specific pyroptosis activation in AD.